

Real-time holographic microscope with nonlinear optics

Ervin Goldfain

Welch Allyn Inc.

ABSTRACT

The paper reveals the schematic of a real time holographic microscope featuring a phase conjugate mirror for retroreflection and a scanning module. The instrument is provided with Epi- and Dia- brightfield capabilities, video/photosensing output and optional optoelectronic processing.

An analysis of the real time restoration process in comparison with conventional holography is presented. The paper reviews the merits and drawbacks of the setup and concludes with a brief discussion on 2D scanning options.

1 INTRODUCTION

We examine below an application of the so-called photorefractive nearly degenerate four wave mixing (DFWM) to solid state imaging in a typical microscope package. Essentially this concept combines benefits of the self-pumped phase conjugation with those given by point or line object scanning. If certain operational requirements related to an efficient phase conjugation, image capture and processing are met, such a setup can deliver real-time holographic images featuring several advantages over conventional or holographic microscopy.

2 ARRANGEMENT DESCRIPTION

As known from literature^{1),2)} a major benefit of using photorefractive crystals to generate DFWM over other similar techniques lies in the low power input (μW) required to activate the self-pumped conjugation. Furthermore if a frequency shifter is used to slightly detune the pump wave, intensity gain in the conjugate beam can be achieved (up to $8..12 \text{ cm}^{-1}$ exponential gain coefficient).

Referring to fig.1 DL stands for a narrow band laser diode, SM is the scanning module C is a collimator lens, NDF a set of neutral density filters, P a s-polarizer plate BS parallel beamsplitters, M high reflectivity mirrors, PM piezomirror, LT light trap D aperture iris, O the object specimen having an unknown transmission function, OS is the objective slider containing objective Ob, PC the phase conjugator consisting of photorefractive crystals such as $\text{B}_{12}\text{SiO}_{20}$, BaTiO_3 , LiNbO_3 or similar, G glass plates A/R coated, DP stands for the recording plane containing appropriate holographic film or a combination of nonlinear masks/substrates or optional video sensors/high resolution photodetector array, A is an amplifier, DE digital electronics and μP is the system microprocessor.

3 CONSTRUCTIVE CONSIDERATIONS

A parallel beam of light delivered by C is split into two components namely the reference pump wave (E_p) and the weak object wave (E_1). The latter coherently illuminates a selected point of line object after being deflected by SM and focussed by the objective Ob. The mirror M_1 creates the readout beam (E_2) and the conjugate beam (E_c) counterpropagates to E_1 ($k_c = -k_1$). The applied electric field E_0 controls the drift velocity and the beam coupling process. Using the piezomirror, frequency of oscillation inside the crystal volume is slightly shifted with respect to pump wave frequency to accomplish quasisonant cavity conditions. The end result is that both fringe spacing

and grating velocity are being optimized¹⁾. Signal photodetection is performed at a location conjugate to the object plane via BS₃ (unit magnification). Frame information can be optionally stored, displayed, magnified or manipulated with appropriate electronic hardware.

The basic setup may be designed in several configurations as shown in fig.1 to fig.4:

1. standard
2. Fourier transform holography
3. confocal scanning
4. object beam steering

Main functional features of the approach are reviewed below:

- a) To change from transmission to reflection, the illuminator module (DL,C,SM,P,NDF) is either swung around an horizontal axis coplanar with the object plane or slid along the upper section of the microscope. When doing so mirror M₂ is manually or automatically flipped in BS_{1,2} must be driven also to the right orientation.
- b) To switch from one arrangement to another, the objective slider is pulled out and locked in the desired location.
- c) The fixed transmission NDF may be substituted by a pair of crossed linear polarizers having variable relative orientation. However it is very likely that image degradation will in this case occur due to local birefringence along the illumination and observation paths.
- d) Photorefractive amplification and lack of crosstalk among interacting beams depend on the applied electric field E₀, incident beam ratio E₀/E₁ as well as on pump beam ratio E₂/E₀. Significant gain requires use of a cascade of two phase conjugators. Tradeoffs between amplification and signal-to-noise ratio + system complexity are to be considered.
- e) Captured image exhibits low sensitivity to object speckle³⁾.
- f) The setup is compatible with conventional optical contrast enhancement techniques available for microscopy (phase contrast, Hoffman modulation). In a broader interpretation, coherent optical processing may be employed to sense phase objects, to evaluate scale/orientation and intensity features or to perform pattern sampling with wedge - ring detection⁴⁾.
- g) Observation of fast changes of the specimen (against steady background) such as crystal growing or bacterial monitoring can be also implemented. In this case the setup takes advantage of fast response scanning provided by either acousto-optical or confocal deflection as well as time-delaying features offered by phase conjugation. Pulsations of the conjugate beam are induced via time-varying the electric field across the crystal⁵⁾.
- h) Besides electronic edge detection, contrast enhancement for low transmission objects is also a potential capability. It is accomplished by swinging out NDF and closing the iris D to increase object beam intensity and attenuate the pump beam. As a result the reconstructed image displays a specific amplitude modulation in phase with specimen's minute details⁵⁾.

Limitations of the setup relate to the following:

- a) Illumination has to be done using coherent narrow band radiation.
- b) No optical magnification is available as in conventional or holographic microscopy.
- c) If object beam steering is achieved with electrooptic modulators, output linearity usually requires 1/4 waveplates in the path.
- d) The degree of optoelectronic complexity is comparable to confocal scanning instrumentation.

It is also known that the time required to obtain a fully developed wave mixing process is a function of incident beam intensity. Thus no instantaneous image reconstruction is possible.

4 ANALOGY WITH FOURIER TRANSFORM IMAGING AND TWO STEP HOLOGRAPHY

The physical process of creating a volume grating inside the photorefractive crystal is equivalent to hologram recording. The refractive index modulation contains the product of reference and object beam amplitudes and can be represented as ⁶⁾ :

$$n = n_0 + [(n/2) \exp(i\phi) E_{01}^* E_{0p} / (E_{01}^2 + E_{0p}^2) \exp(-iKr) + c.c.] \quad (1)$$

where $K = k_1 - k_p = 2\pi/\Lambda$, Λ = period of fringe pattern, ϕ = relative phase shift between the index grating and the intensity pattern, E_{01} and E_{0p} = electric field amplitudes. The solution of Kukhtarev's model for a two-beam coupling with a moving grating leads to an optimum fringe spacing:

$$\Lambda_{opt} = 2\pi E_0 N_A^{-1} (-\mu \epsilon_0 \epsilon_1 \gamma e)^{-1/2} \quad (2)$$

where N_A is acceptor density, γ the recombination coefficient, E_0 stands for the applied electric field and μ for charge carriers mobility. For instance following numerical values apply to the $Bi_{12}SiO_{20}$ when $E_0 = 10 \text{ kV.cm}^{-1}$:

$$\Lambda_{opt}^{-1} = 35 \text{ mm}^{-1}, N_A = .95 \times 10^{22} \text{ m}^{-3}, \mu = 10^{-5} \text{ m}^2 \cdot \text{V.s}^{-1} \quad (3)$$

Hologram recording is generated by steady wave mixing of E_1 and E_2 while real-time reconstruction is initiated by E_2 . An analogy with side band Fresnel holography in reflected light yields the following lateral magnification of the reconstructed image ⁷⁾ :

$$m = [R_1 / (R_1 + s_1) - k_2 s_1 / (k_p R_2)]^{-1} \quad (4)$$

in which s_1 is the distance object to hologram and R_1, R_2 are the curvature radii for illumination and readout. Since $R_1, R_2 \rightarrow \infty$ (plane waves) the above relation gives unit magnification.

This circumstance indicates that the phase conjugator PC operates as a Fourier transform lens in itself since the conjugate beam is a time-reversed replica of the object beam.

Assuming:

$$1/z_1 + 1/z_2 = 1/f \quad (5)$$

$$b \gg 2f/k_1 \quad (6)$$

where z_1, z_2 are the finite conjugates with respect to equivalent lens principal planes and b is crystal width, and imposing $z_1 = z_2$ one obtains the amplitude distribution in the recording plane as:

$$D(\alpha) = (\text{const}) \cdot A' \cdot F_D(\alpha/\lambda_1 f) \quad (7)$$

in which ⁷⁾:

$$A' = c_1 c_2 \exp(ik_1 \alpha^2 / 2f) \quad (8)$$

$$c_1 = (1 - ik_1 s_2) \cos \theta / 2\pi s_2^2 \quad (9)$$

$$c_2 = (1 - ik_c s_1) \cos \theta / 2\pi s_1^2 \quad (10)$$

$$\cos \theta = s_1 / r = s_1 / [(\xi - x)^2 + (\eta - y)^2 + s_1^2]^{1/2} \quad (11)$$

$$F_D(\alpha / \lambda_1 f) = \int D(\xi) \cdot \exp[-ik_1 (\xi \cdot \alpha) / f] d\xi \quad (\text{Fourier transform}) \quad (12)$$

ξ, η = coordinates in the object plane

x, y = coordinates in the aperture plane of the conjugator (13)

α, β = coordinates in the detector plane

To test the validity of the above comparison, one can place a target grating (with a well defined spatial frequency and transmission) in the object plane and monitor the detector response. Amplitude distribution given by (7) becomes the calibration gauge of the phase conjugator.

The arrangement presented in fig. 2b operates with an intermediate objective lens placed between BS₃ and PC. Because the returning beam forms an image after passing through the lens, all its phase distortions are being removed (the "undoing" theorem of phase conjugation³). This layout is optically similar to the Fourier transform holographic setup in which both recording and reconstruction are performed with the same objective. Using the so-called reference point source on axis, the complex distribution in the lens transform plane yields (refer to fig. 5):

$$\psi(\xi) = \delta(\xi) + D(\xi - \xi_0) \quad (14)$$

$$\tilde{\psi}(x / \lambda_1 f) = (\text{const.}) A' [1 + F_D(x / \lambda_1 f) \exp[-ik_1 (\xi_0 x) / f]] = F_\psi(x / \lambda_1 f) \quad (15)$$

in which $\tilde{\psi}$ represents the aperture transform and $\delta(\xi)$ the delta function associated with the pinhole aperture. From (15) the resultant complex distribution in the detector plane can be written in terms of convolution product involving the lens and the phase conjugator:

$$\psi(\alpha) \sim \delta(\alpha) + D^*(\alpha) \otimes D(\alpha) + D[-(\alpha + \xi_0)] + D^*(\alpha - \xi_0) \quad (16)$$

5 SCANNING OPTIONS

Several alternatives are available for object point or line scanning:

1. galvanomirror
2. polygon scanning
3. acoustooptic deflection
4. confocal scanning
5. object beam steering (2D array)

A comparative evaluation between these options is briefly presented below :

-galvanomirror and polygon scanning potentially increase instrument sensitivity to unbalanced mechanical vibration.

-acoustooptic scanning implies several technical limitations such as:

a) Bragg diffraction produces an angular spread of beam energy among various orders.

It can be shown that $\Delta\phi \sim (1/k_1 v_s) \Delta f$ is the zero order deflection while $\delta\phi \sim (1/k_1 d)$, in which d stands for beam diameter, δ is the angular spread. In these formulas f and v_s are the sound frequency and group velocity, respectively. Therefore high resolution requires high frequency modulation and large beam apertures.

b) a Doppler shift in beam frequency, equal in magnitude with the sound frequency (75.. 100 MHz), is to be expected. This may create resolution difficulties when minute frequency increments are sought to be achieved with the piezomirror.⁸⁾

c) Acoustooptic scanning exhibits nonlinearity in the deflected power ($\sim \sin^2 A_s$, where A_s is the sound amplitude).

d) anamorphic optics is required to deliver a "sheet-like" object beam to the scanner⁹⁾ -The confocal scanning arrangement is illustrated in fig.3 (DIA- option only). The basic feature is the Nipkow spinning disk matching point sources in the illumination path with the corresponding detector pinholes in the recording path. The technique is suitable for high resolution viewing of reflective surfaces (ceramics and metals), defect evaluation in semiconductors and in all applications where blocking the scattered light from an irregular specimen is essential. A tradeoff analysis is necessary to set optimum balance between beam power and pinhole size.

-Wavefront steering takes advantage of a two-wave mixing geometry with amplification in the object beam. The reference wave steadily exchanges energy inside a BaTiO₃ crystal with a selected "pixel" beam emerging from a 2D array of electrooptic shutters.

Referring to fig.4, object scanning across the X-direction is implemented with appropriate optical multiplexing (array of fibers and microlenses).

5 SUMMARY

A preliminary investigation on a novel holographic microscope featuring nonlinear retro reflection has been presented. Making use of low power DFWM properties of photorefractive crystals, the setup explores new grounds in the field of real-time image recording. Potential "first order" benefits/drawbacks and design considerations were discussed. It is our hope that further theoretical and experimental developments will provide additional insight to this promising concept.

6 REFERENCES

1. J.P.Huignard, H.Rajbenbach, Ph.Refregier, L.Solymar, "Wave mixing in photorefractive bismuth silicon oxide crystals and its applications", OE, vol.24/4, july-august 1985.
2. Pochi Yeh, Arthur E. Chiou et al., "Photorefractive nonlinear optics and optical computing", OE, vol.28/4, april 1989.
3. Fisher R., "Optical phase conjugation", SPIE's OE LASE'90 (short course notes), 1990.
4. Casasent D., "Coherent optical pattern recognition: a review", OE, vol24/1, jan.1985
5. Pepper D., Feinberg J., Kukhtarev N., "The photorefractive effect", Scientific American, october 1990.
6. Vinetskii V.L., Kukhtarev N. et al., "Dynamic self-diffraction of coherent light beams" Sov. Phys.Usp. 22,742-757, 1979.
7. DeVelis J.B., Reynolds G.O., "Theory and applications of holography", Addison-Wesley Co., 1967.
8. Young M., "Optics and lasers", Springer Verlag, 1987.
9. Korpel A., "Acousto-Optics", Applied Optics and Optical Engineering, vol.6, Academic Press, 1980.

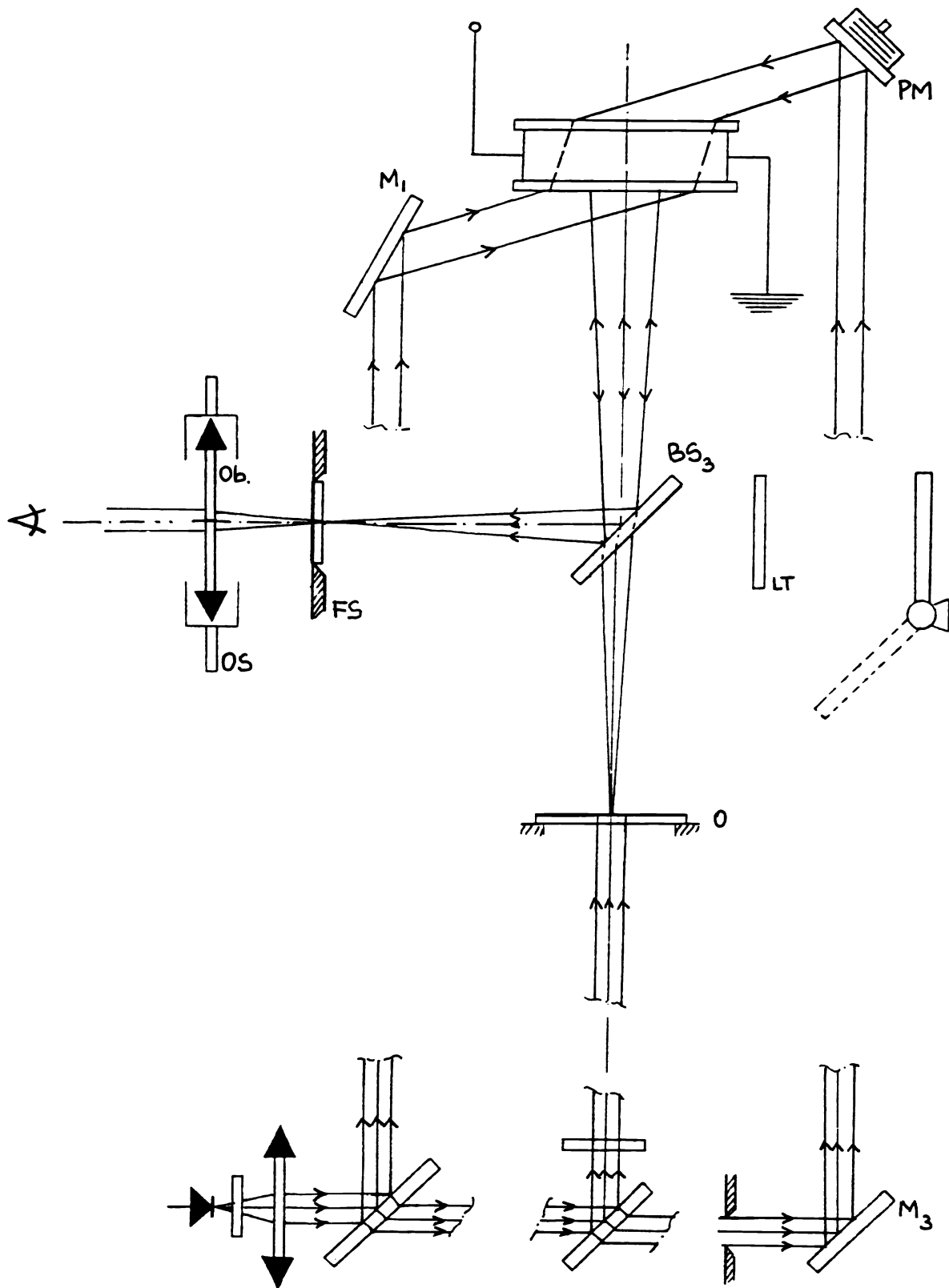


fig. 2a

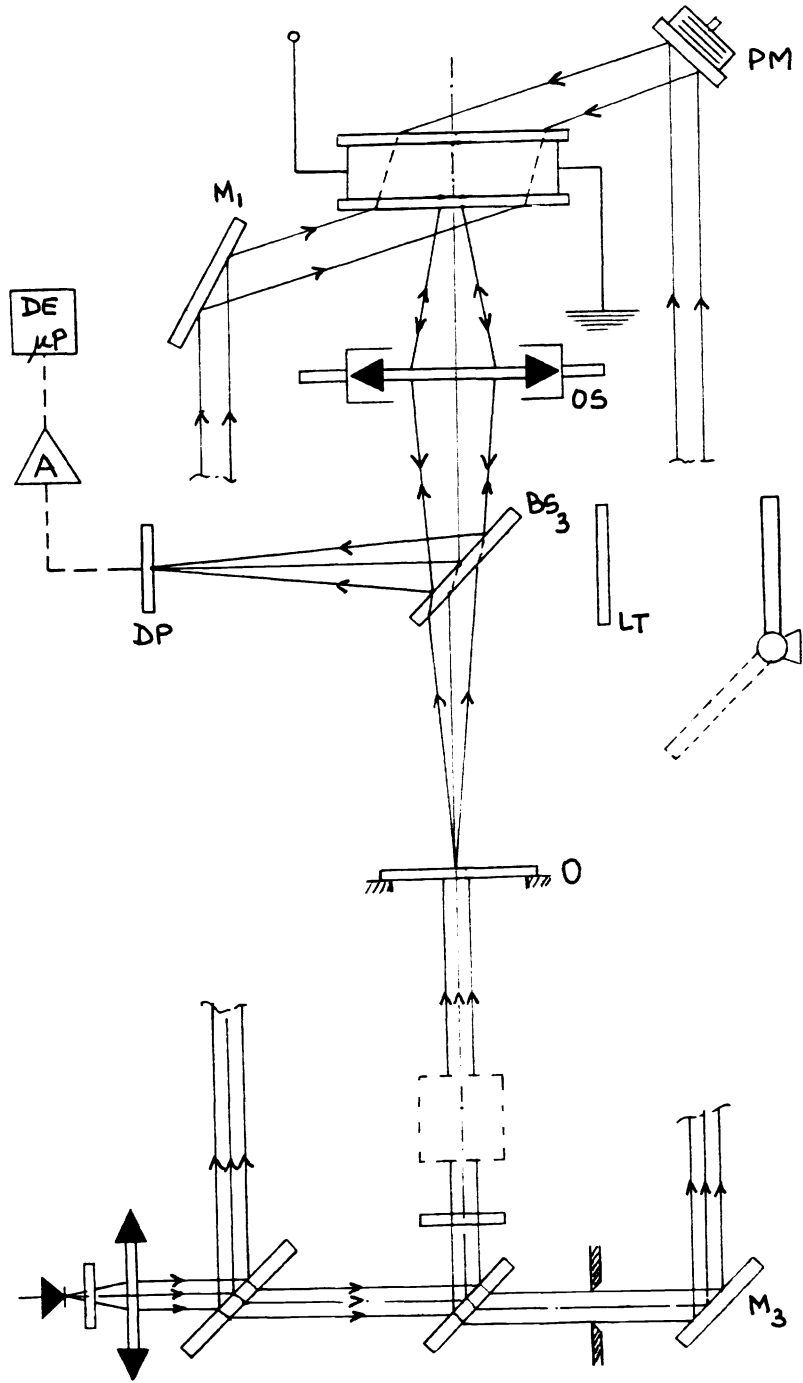


fig.2b

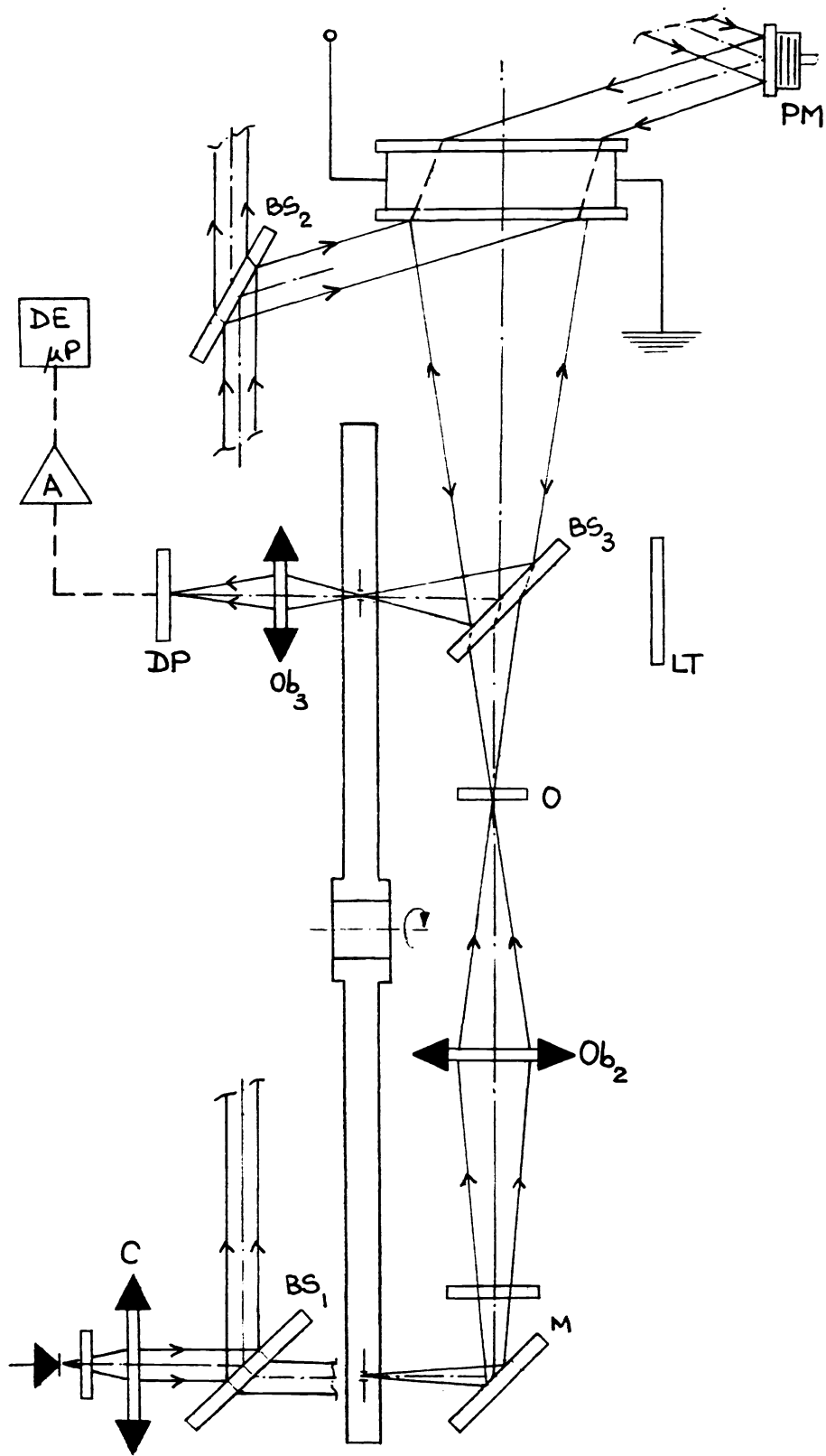


fig.3

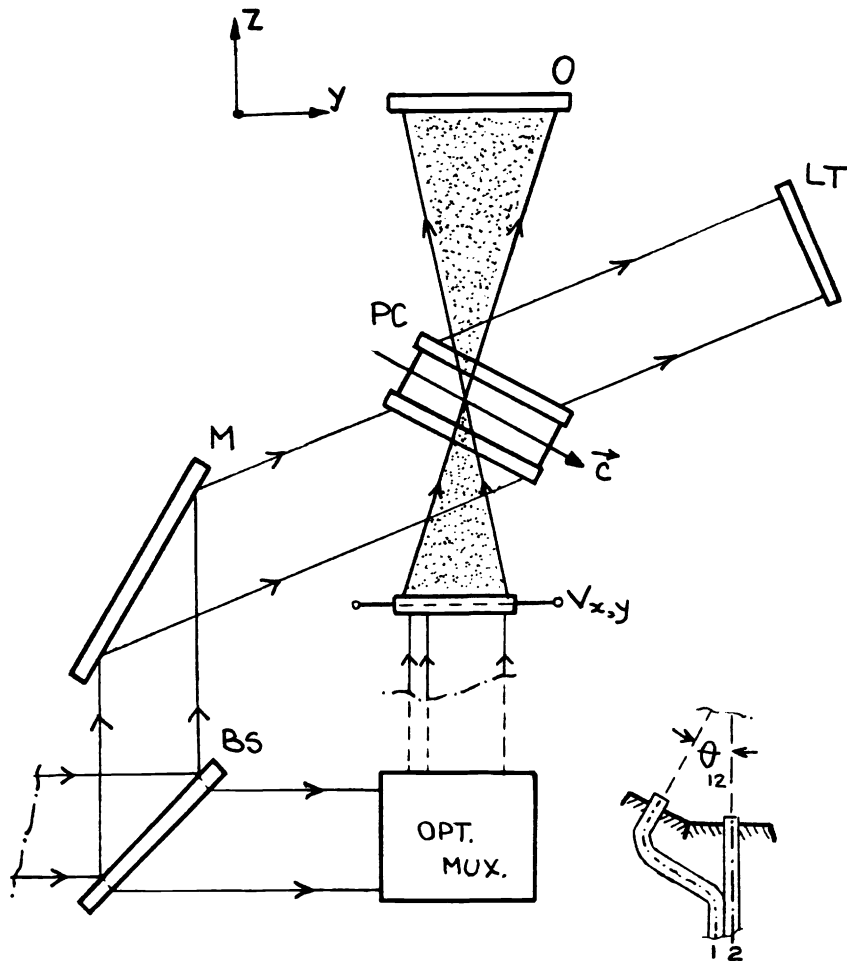


fig. 4

